

ALEJANDRO FERNÁNDEZ GÓMEZ, MACIEJ SUŁOWICZ, TADEUSZ J. SOBCZYK*

THE INFLUENCE OF MECHANICAL FAULTS ON INDUCTION MACHINES WITH ELECTRICAL FAULTS

WPŁYW USZKODZEŃ MECHANICZNYCH W SILNIKU INDUKCYJNYM NA OCENĘ USZKODZEŃ ELEKTRYCZNYCH

Abstract

The study of the interaction between faults of different natures is a crucial step for the development of effective systems for fault detection. The analysis of the electrical signals using the actual motor current signature analysis (MCSA) techniques may lead to different results and, as a consequence, an incorrect diagnosis of the fault due to the fact that the non-linear interactions between both faults are difficult to predict with high precision. The relationship between the electrical and mechanical components has been extensively studied in the past, but despite the progress made, the introduction of new control systems or the nonlinearities presented in the electrical machine, still makes it hard to diagnose faults. The study below attempts to show the evolution of the induction motor signatures when electrical and mechanical faults occur simultaneously. The Fourier analysis of the signatures presented in this paper indicates that the typical analysis carried out to diagnose the state of the electrical machine may be interpreted as an indicator of a different type of fault.

Keywords: induction motors, broken bar, mechanical fault, Fourier, Simulink

Streszczenie

Badanie interakcji występujących między efektami różnej natury uszkodzeń jest kluczowym krokiem w rozwoju efektywnych systemów diagnostycznych do wykrywania uszkodzeń maszyn indukcyjnych. Analiza prądu stojana z wykorzystaniem metody MCSA (*Motor Current Signature Analysis*) może prowadzić do różnych wyników i w konsekwencji do błędnego rozpoznania uszkodzenia. Spowodowane jest to tym, że nieliniowe interakcje pomiędzy różnymi uszkodzeniami są trudne do przewidzenia i oszacowania z wystarczającą dokładnością. Relacje między charakterystycznymi komponentami uszkodzeń elektrycznych i mechanicznych zostały już dość dobrze zbadane w przeszłości, ale mimo to wciąż sprawiają trudności w zdiagnozowaniu poszczególnych uszkodzeń. Zawarte w artykule wyniki analiz stanowią próbę ukazania rozwoju charakterystycznych składowych w widmach prądu stojana silnika indukcyjnego podczas równoczesnego występowania zakłóceń elektrycznych i mechanicznych. Przedstawione w pracy analizy widmowe charakterystycznych cech tych uszkodzeń dowodzą, że typowa analiza przeprowadzona na podstawie metody MCSA może wpłynąć na błędne określenie stanu maszyny i złą interpretację uzyskanych wyników przez wskazanie innego typu uszkodzenia niż to, które rzeczywiście wystąpiło.

Słowa kluczowe: silnik indukcyjny, uszkodzony pręt klatki, uszkodzenie mechaniczne, Fourier, Simulink

DOI: 10.4467/2353737XCT.15.026.3826

* M.Sc. Alejandro Fernández Gómez, Ph.D. Eng. Maciej Sułowicz, Prof. D.Sc. Ph.D. Eng. Tadeusz J. Sobczyk, Institute on Electromechanical Energy Conversion, Faculty of Electrical and Computer Engineering, Cracow University of Technology.

1. Introduction

The fault diagnosis of electrical motors is a topic frequently discussed in relation to industrial solutions, especially in those cases in which high power machines run the production process. The scientific community together with industry have dealt with this challenge for many years now, but there is still no global solution available due to the evolution of the industry. For instance, the development of new drives for electrical motors brought new difficulties in the condition monitoring and fault diagnosis.

It is well known that the sideband components around the fundamental frequency $(1 \pm 2s)f_0$ for $k = \pm 1, \pm 2, \pm 3 \dots$ are typically used as an indicator of electrical faults and mechanical faults, and they depend on the torque demanded by the load.

However, the study and analysis of those components have been considered insufficient to detect faults in some cases, in which authors suggested complementary studies of other components of the stator currents, electromagnetic torque or rotor speed [1–4]. In [5], the authors suggest the use of the component at a frequency of $(5 - 4s)f_0$ in order to detect rotor faults due to the fact that this component increases with the number of broken bars whereas it remains almost unchangeable for the inertia of the motor-load unit as well as for supply voltage distortion or unbalance. In [6], the components around the principal slot harmonic PHS have been considered in order to detect the mechanical unbalance.

Nevertheless, those studies have not considered the possible effects on the frequency magnitudes that may happen when two of these faults occur simultaneously due to the interactions existing between electrical and mechanical components of the electrical machine.

In large scale motors at nominal conditions, the slip is rather small and the frequency sidebands are in a range of few Hertz. However, low frequency components are also a typical effect when a fault occurs in turbo-machinery, for instance, surges in centrifugal compressors. Surge is a phenomenon in which mass flow oscillations are produced due to the rise of pressure and rotational speed of the compressor, causing and alternating the component in the compressor's torque [7]. This phenomenon appears when the operation point of the compressor exceeds the stability limit in the compressor's map and may cause severe damage to the machine. In big compressors, i.e. 7–8 MW power, the surge frequency is about 1–2 Hz [8].

The objective of this work is to show the alterations produced in the frequency spectrum, when the above faults affect the whole system at once, of the sideband components around the main frequency, considering resonances due to the fact that characteristic frequencies of both faults may be equal. The load, the inertia of the system, the magnitude and phase of the mechanical load and the severity of the rotor fault have been considered.

The results have shown big differences in the magnitudes of sidebands as a function of the mechanical load conditions. Simulink has been selected as a platform to develop faulty dynamic models of induction motors (IM) based on the effect of main magneto-motive forces.

2. Models

2.2. Internal electrical fault – Broken Bar

A broken or incipient broken bar is one of the common faults in induction motors. When rotor defects appear, the symmetry is lost inducing additional components in the motor current the frequency of which is $(1 - 2s)f_0$. This frequency is responsible for the appearance of a torque ripple at a frequency of $2sf_0$. The ripple in the torque creates a new current in the stator windings at a frequency of $(1 + 2s)f_0$, hence, a new magnetic field arises with a frequency respect to rotor $3sf_0$. The interaction between magneto motive forces of the stator and rotor (MMF's) due to cage asymmetry, give rise to frequency components $(1 \pm 2s)f_0$ for $k = \pm 1, \pm 2, \pm 3 \dots$ in the current spectrum. The magnitude of the components is lessened more and more for the inertia of the machine. Because of that, fault detection is focused on $(1 \pm 2s)f_0$.

The asymmetry of the cage is modeled increasing the resistance of the element affected by the fault. The change of the resistance is typically estimated by an increase of 20 times the initial value, therefore, an additional term of the rotor resistance will appear. It is well known that asymmetry and symmetry coefficients are used to indicate the increase of the cage resistance [9]. The use of this model is limited as it is only valid for those cases in which the slip remains closer to the nominal slip, otherwise, the matrix of inductance should also be changed.

The model for the internal electrical fault is described as follows:

$$\frac{d}{dt} \begin{bmatrix} \Psi_{sd} \\ \Psi_{sq} \\ \Psi'_{rd} \\ \Psi'_{r'q} \end{bmatrix} + \begin{bmatrix} -\omega_s \cdot \Psi_{sq} \\ \omega_s \cdot \Psi_{sd} \\ -\omega_r \cdot \Psi'_{r'q} \\ \omega_r \cdot \Psi'_{rd} \end{bmatrix} + [\mathbf{R}] \cdot \begin{bmatrix} i_{sd} \\ i_{sq} \\ i'_{rd} \\ i'_{r'q} \end{bmatrix} = \begin{bmatrix} u_{sd} \\ u_{sq} \\ 0 \\ 0 \end{bmatrix} \quad (1)$$

$$[\mathbf{R}] = \begin{bmatrix} R_s & 0 & 0 & 0 \\ 0 & R_s & 0 & 0 \\ 0 & 0 & R_r^p \cdot (1 + k_s + k_{as} \cdot \cos(2 \cdot \gamma_r)) & R_r^p \cdot k_{as} \cdot \sin(2 \cdot \gamma_r) \\ 0 & 0 & R_r^p \cdot k_{as} \cdot \sin(2 \cdot \gamma_r) & R_r^p \cdot (1 + k_s - k_{as} \cdot \cos(2 \cdot \gamma_r)) \end{bmatrix} \quad (2)$$

$$\begin{bmatrix} \Psi_{sd} \\ \Psi_{sq} \\ \Psi'_{rd} \\ \Psi'_{r'q} \end{bmatrix} = \begin{bmatrix} L_{\sigma s} + L_m & 0 & L_m & 0 \\ 0 & L_{\sigma s} + L_m & 0 & L_m \\ L_m & 0 & L_{\sigma r} + L_m & 0 \\ 0 & L_m & 0 & L_{\sigma r} + L_m \end{bmatrix} \cdot \begin{bmatrix} i_{sd} \\ i_{sq} \\ i'_{rd} \\ i'_{r'q} \end{bmatrix} \quad (3)$$

where:

- Ψ_{sd} – the stator and rotor fluxes in the d - q components,
- i_{sd} – the stator and rotor currents,
- $w_{s,r}$ – the stator and rotor speed,
- u_{sd} – the stator voltages,
- R_s – the stator resistance,
- R_r^{1p} – the equivalent rotor resistance,
- γ_r – the rotor rotational angle,
- $L_{\sigma s,r}$ – the stator and rotor leakage inductance,
- L_m – the mutual inductance,
- k_s – the symmetry factor,
- k_{as} – the asymmetry factor.

For the purpose of clarity, the equations used have been transformed into components d - q and stator and rotor fluxes have been chosen as state variables.

One broken bar has been considered in the analysis, hence, the corresponding value of k_s and k_{as} is 0.0291.

2.3. Generic Mechanical Fault

Electrical motors are the main component of a large variety of industries connected to a wide range of machinery. Their functionality is often affected by a malfunction in the load causing severe damage if it is not detected quickly, especially in high power machines. For example, an unbalanced rotation shaft due to a fault in the gearbox or a broken ball in a bearing creates an additional torque and in some cases, an asymmetry in the air-gap.

The reaction of the induction motor due to this type of fault can be studied through a set of two mechanical equations together with additional torque components, time or angle dependent.

$$J \frac{d\omega_r}{dt} + D \frac{d\varphi}{dt} = T_{ele} - T_z \quad (4)$$

$$\frac{d\varphi}{dt} = \omega_r \quad (5)$$

where:

- J – the moment of inertia of the rotor plus the load,
- D – the dumping term,
- T_{ele} – the electromechanical torque,
- T_z – the resistive torque in shaft,
- φ – the geometrical angle of the rotor,
- ω_r – the mechanical speed of the rotor.

Usually, the dumping term can be neglected.

In order to study the effects of a generic mechanical fault, T_z has been defined as the sum of a constant component plus an alternating component T_{AC} , in which the main harmonic has only been considered, with adjustable frequency f_z . The amplitude of T_{AC} has been defined under the assumption of the same effects over the electromagnetic torque as the broken bar.

$$T_z' = T_z + T_{AC} \cdot \sin(2\pi f_0 + \alpha_z) \quad (6)$$

Where f_0 is the net frequency and α_z is the phase of the mechanical oscillation.

3. Results

In the previous sections, the relationship between the two sideband components close to the main net frequency is explained. The objective of the experiments is to clarify what the changes in magnitude are of the two components bringing light to the following challenges:

- If the mechanical frequency f_{BB} with a value of $2s f_0$ creates additional components at the same frequency as the broken bar, what can be expected in terms of magnitude when both faults occur simultaneously?
- The mechanical fault depends on the magnitude of the oscillating component as well as the phase. Considering frequencies f_z and f_{BB} have the same value, what would the behavior of components be if the mechanical fault phase is different?

Experiments were conducted in a 4 kW motor and the results are discussed in the following sections. However, the simulation results were obtained for a 2000 kW motor with the purpose of confirming that the same consequences can be expected independently of the motor size. Discrete induction machine models based on the Euler forward method were used in Simulink with a time step of $1e-5$ (Simulation parameters: fix step and discrete solver). The following induction motor with the following rated data was chosen: $P_N = 2000$ kW; $n_N = 2980$ rpm; $U_N = 6$ kV; $I_N = 227$ A; $p = 1$; $N = 36$ rotor bars; $J = 34$ kgm².

For the benefit of clarity, the Fourier spectrum of the stator phase currents was referred to the magnitude of the 50 Hz component (rms * $1e-5$).

3.1. Evolution of Broken Bar component magnitude

A ripple with a characteristic frequency can be observed in the stator currents due to both types of faults. The simulations were carried out considering the same fault severity. Therefore, the amplitude of the mechanical alternating component produces a ripple in the electromagnetic torque equivalent to the broken bar effects. The following figures and tables show the evolution of $(1 \pm 2s)f_0$ components magnitude.

The load of the machine is one of the factors with more influence on the diagnosis and evolution of certain types of fault. For instance, the magnitude of the sidebands due to broken bar changes according to the load. The analysis has been carried out for different load scenarios considering the phase angle α_z equal to zero, loaded with 100%, 75% and 50% of the nominal torque. On the other hand, for greater slips, fluctuations in the speed reflected in

the $(1 - 2s)f_0$ component disappear as well as the component itself, hence, the influence of the machine inertia was also considered.

A filter was applied and the net frequency removed from the Fourier spectra of the stator phase currents.

Figures 1–3 show changes in the magnitude of the $(1 \pm 2s)f_0$ components in the linear scale as a function of the mechanical fault frequency f_z , which decreased from 4.5 Hz to 1.5 Hz, and the moment of inertia equal to twice the inertia of the induction motor (notice that red indicates the frequency component due to mechanical fault).

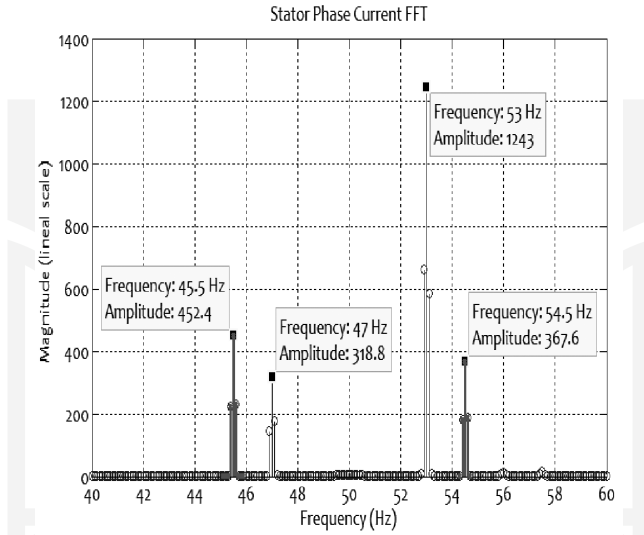


Fig. 1. Fourier Spectra of Phase current A: 100% Nominal torque and $f_z = 4.5$ Hz

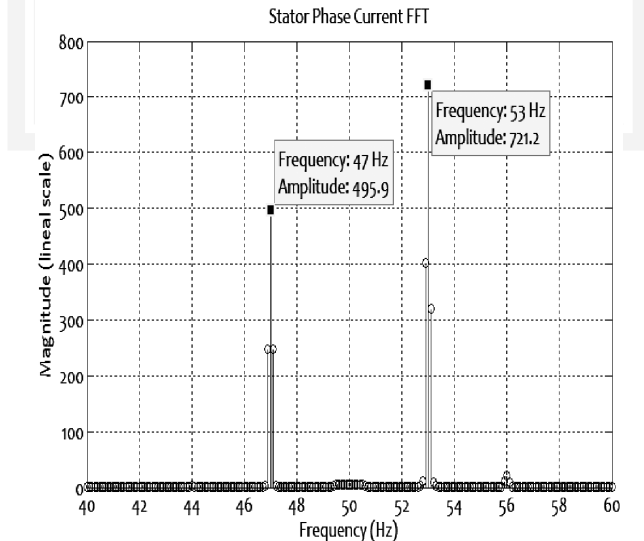


Fig. 2. Fourier Spectra of Phase current A: 100% Nominal torque and $f_z = 3$ Hz

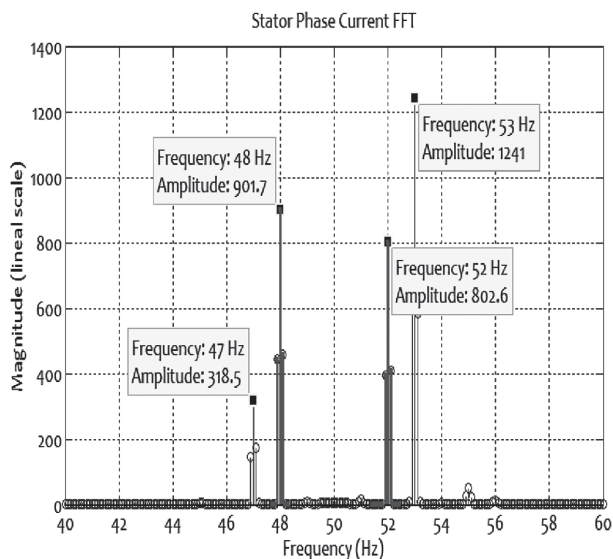


Fig. 3. Fourier Spectra of Phase current A: 100% Nominal torque and $f_z = 2$ Hz

Table 1 completes the analysis showing the changes of the frequencies do not included in the previous figures.

Table 1

Magnitude of $(1 \pm 2s)f_0$ component for inertia twice the motor inertia

f_{BB}/f_z	4.5 Hz	4 Hz	3.5 Hz	3 Hz	2.5 Hz	2 Hz
47 Hz 100% Tn	318.77	318.76	318.75	<u>496</u>	318.53	318.46
53 Hz 100% Tn	1242.55	1242.5	1242.34	<u>721.07</u>	1241.9	1241.22

It can be noted that the magnitude of the components only change considerably when the mechanical frequency is equal to the broken bar frequency independent of the load. In case of a different load, the same tendency can be observed. However, this effect is attenuated when the inertia of the systems is increased. In addition, the magnitude of the mechanical fault components increased as expected.

3.1. Evolution of Broken Bar component magnitude due to phase changes

According to the previous experiment, the magnitude of the sidebands $(1 \pm 2s)f_0$ changes if the frequency of both faults is equal. The second simulations explore how the phase may also change the magnitude.

Changing the phase of the alternating component of the mechanical load from 0 to 2π in ten steps, Fig. 4 shows the effects on the component's amplitude for equal severity faults, nominal torque, J twice the motor inertia and $f_z = 3$ Hz.

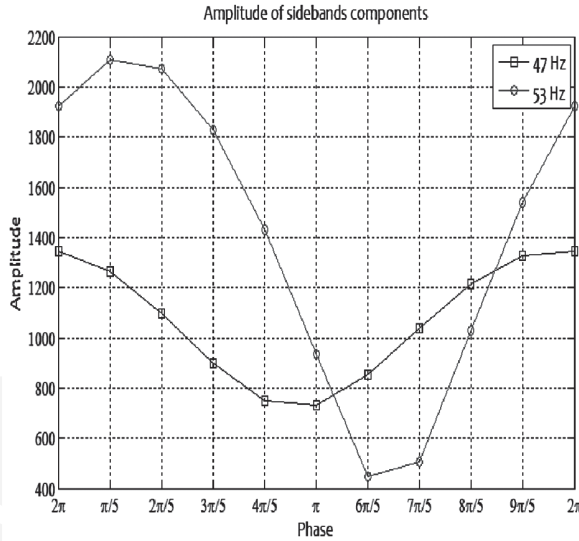


Fig. 4. Evolution of Sideband's Amplitude regarding mechanical phase

The alternation between both components which has the greater value due to phase changes can be observed. A modulation of low frequency of the stator phase currents has also been observed in the simulations. The resolution of the Fourier spectra used is 0.1 Hz and the component of that modulation could not be observed in the spectrum. Figure 5 shows the modulation (note the time scale). Figure 6 shows the presence of the ripple at 3 Hz due to fault. Figure 7 shows that the modulation is also present if f_z suffers slight changes (3.1 Hz) and it is divided in two: a) the left side shows the ripple at frequency 3.1 Hz as Fig. 6; b) the right side shows the modulation of the stator currents as Fig. 5.

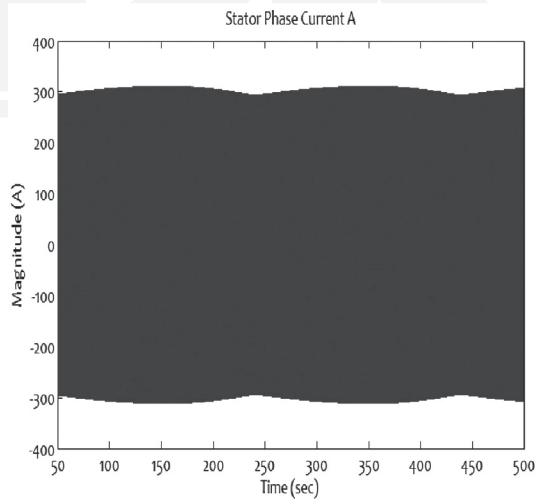


Fig. 5. Phase current modulation $f_z = 3$ Hz

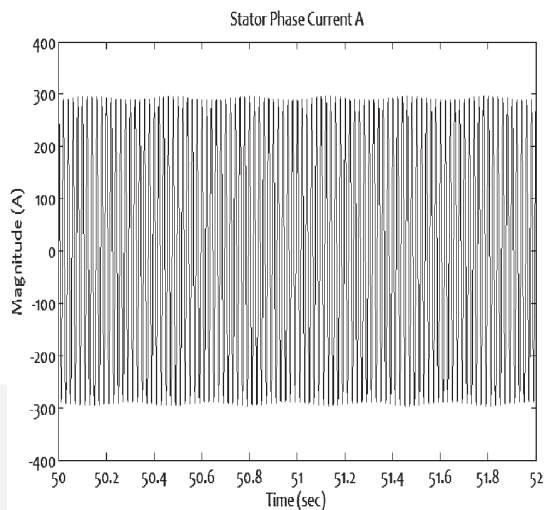


Fig. 6. Phase current modulation $f_z = 3$ Hz zoom

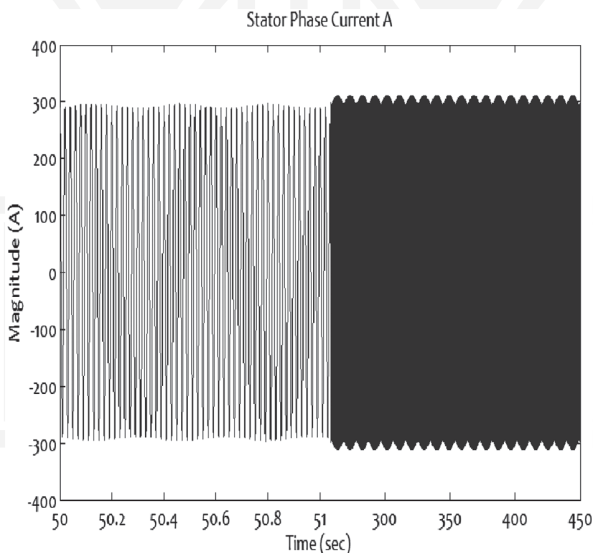


Fig. 7. Phase current modulation $f_z = 3.1$ Hz zoom

3.3. Experimental results

A qualitative analysis of the results shown in subchapter 3.1 was carried out with a motor of rated data $P_N = 4$ kW, $n_N = 1480$ rpm, $U_N = 400$ V, $I_N = 2.6$ A, $p = 2$, $N = 28$ rotor bars and $J = 0.019$ kgm². The mechanical fault was created controlling the field winding current of a DC motor by a power electronic converter, hence, the resistive torque applied to the motor for a given frequency f_z .

Figures 8–11 show the current spectrum for the following faults – one broken bar and one broken bar plus mechanical fault with an amplitude of 10% of the nominal torque and frequencies f_z equal to 6 Hz, 5.2 Hz and 4 Hz respectively.

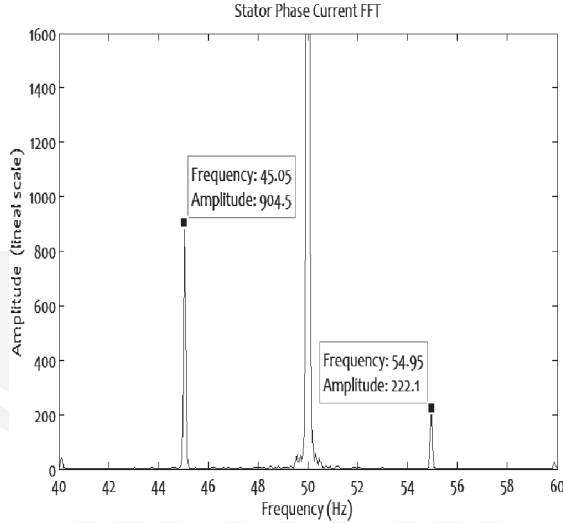


Fig. 8. Fourier Spectra of Phase current A: Broken Bar at 100% Nominal torque

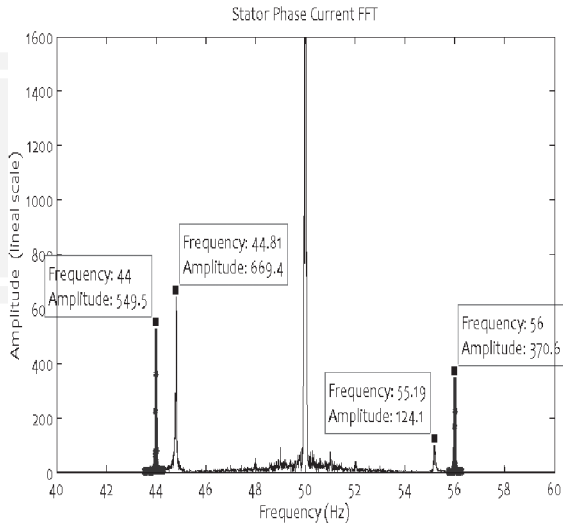


Fig. 9. Fourier Spectra of Phase current A: Broken Bar and $f_z = 6$ Hz

The evolution of the sidebands $(1 \pm 2s)f_0$ agrees with the simulation results. The amplitude of the broken bar is lower if the mechanical fault arises (Fig. 8). The amplitude of both mechanical components is greater when f_z is lower than f_{BB} as it has been shown in Figs. 1 and 3. Finally, if f_z reaches the value of f_{BB} , the difference between amplitudes of both sidebands, resulted from the sum of both fault effects, is reduced as it has been shown in Fig. 2.

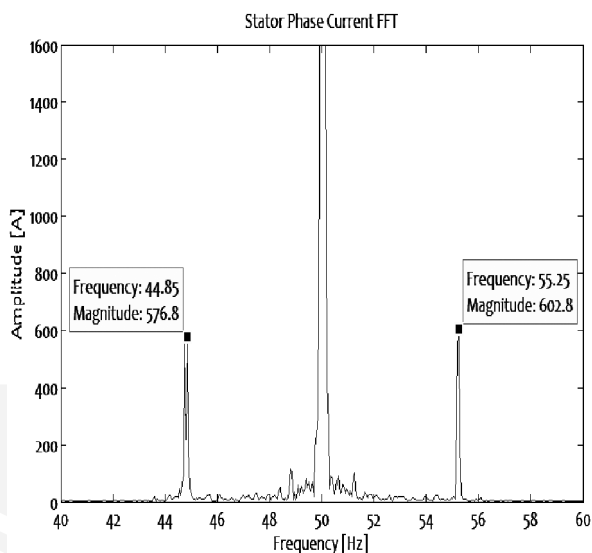


Fig. 10. Fourier Spectra of Phase current A: Broken Bar and $f_z = 5.2$ Hz

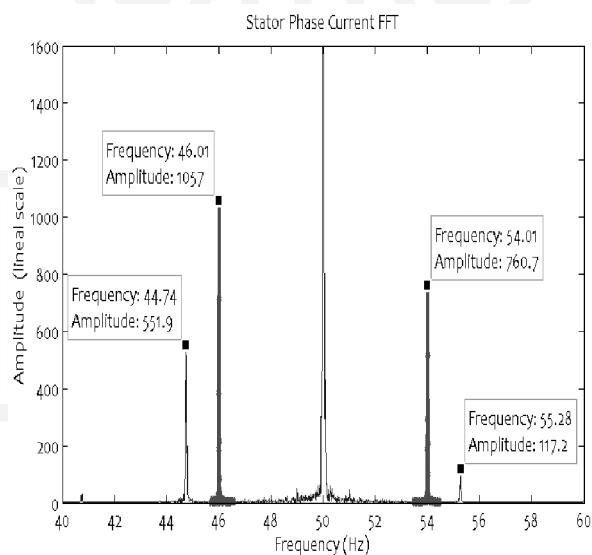


Fig. 11. Fourier Spectra of Phase current A: Broken Bar and $f_z = 4$ Hz

4. Conclusions

The aim of the paper is to study which phenomena occur in the induction motor when two of the commonest faults appear simultaneously – one broken bar and a mechanical fault. The MCSA technique was applied to study the evolution of the sideband frequencies $(1 \pm 2s)f_0$ extensively

used for the diagnosis of both faults. Changes in magnitudes were studied in order to reveal the behavior of the motor. The Fourier spectrum has shown differences regarding the faults applied and load conditions. Simulink was used as a platform for the development of IM models.

Simulations have shown that the magnitude of the sidebands $(1 \pm 2s)f_0$ only changed when mechanical fault frequency f_z reached the same value as the broken bar frequency f_{BB} . The experimental results confirmed, qualitatively, the evolution shown in the simulation results.

According to the simulation results, the phase of the mechanical fault has an important role, leading to possible misinterpretation of the results derived from the IM diagnosis due to changes in the sideband amplitudes.

One of the techniques applied to detect the presence of the broken bar or incipient broken bar in electrical motors consisted of studying the differences between the magnitudes of the two sidebands $(1 \pm 2s)f_0$ establishing global fault indicators [1, 10]. The presence of a mechanical fault produces variations in magnitudes that may alter the value of the indicator leading to incorrect diagnosis.

It is worth mentioning that the high difference between sideband components can be attributed to cases where more than one bar was damaged.

Future research may be focused on studying systems which not only include a model of the electrical machine plus a generic mechanical fault, but also the mechanical load driven, due to the fact that nowadays, industry demands solutions customized for individual systems. The inclusion of electrical machine models in the studies carried out to evaluate failures in turbo-machinery could point out that damage could be increased due to electrical faults and vice versa.

References

- [1] Didier G., Ternisien E., Caspary O., Razik H., *Fault detection of broken rotor bars in induction motor using a global fault index*, Industry Applications, IEEE Transactions, 2006, Vol. 42, No. 1, pp. 79–88.
- [2] Concari C., Franceschini G., Tassoni C., *Discerning mechanical load unbalances from rotor faults in induction machines through current space vector components*, IECON 2010 – 36th Annual Conference on IEEE Industrial Electronics Society, 2010, pp. 2609–2614.
- [3] Bellini A., Concari C., Franceschini G., Lorenzani E., Tassoni C., Toscani A., *Thorough understanding and experimental validation of current sideband components in induction machines rotor monitoring*, IEEE Industrial Electronics, IECON 32nd Annual Conference, 2006, pp. 4957–4962.
- [4] Martins Cunha C.C., Lyra R.O.C., Filho B.C., *Simulation and analysis of induction machines with rotor asymmetries*, Industry Applications, IEEE Transactions, 2005, Vol. 41, No. 1, pp. 18–24.
- [5] Bossio G.R., De Angelo C.H., Pezzani C.M., Bossio J.M., Garcia G.O., *Evaluation of harmonic current sidebands for broken bar diagnosis in induction motors*, Diagnostics for Electric Machines, Power Electronics and Drives, SDEMPED IEEE International Symposium, 2009, pp. 1–6.

- [6] Salah M., Bacha K., Chaari A., *Stator current analysis of a squirrel cage motor running under mechanical unbalance condition*, En Systems, Signals & Devices (SSD), 10th International Multi-Conference, 2013, IEEE, pp. 1–6.
- [7] Giampaolo T., *Compressor Handbook: Principles and Practice*, The Fairmont Press, Inc., 2010.
- [8] Gravdahl J.T., Egeland O., Vataland S., *Drive torque actuation in active surge control of centrifugal compressors*, Automatica, 2002, Vol. 38, No. 11, pp. 1881–1893.
- [9] Fernández Gómez A.J., Sobczyk T.J., *Motor current signature analysis apply for external mechanical fault and cage asymmetry in induction motors*, Diagnostics for Electric Machines, Power Electronics and Drives (SDEMPED), 9th IEEE International Symposium, 2013, pp. 136–141.
- [10] Bellini A., Filippetti F., Franceschini G., Tassoni C., Kliman G.B., *Quantitative evaluation of induction motor broken bars by means of electrical signature analysis*, IEEE Tran. on Ind. Appl., 2001, Vol. 37, No. 5, pp. 1248–1255.

